Time dependence of multiply scattered diffuse ultrasound in polycrystalline media

Joseph A. Turner and Richard L. Weaver
Department of Theoretical and Applied Mechanics
216 Talbot Laboratory
104 South Wright Street
University of Illinois at Urbana-Champaign
Urbana, IL 61801

Abstract

Time domain results are presented for the multiply scattered longitudinal intensity backscattered from a polycrystalline medium. The results are solutions to the ultrasonic radiative transfer equation (URTE), the derivation of which is based upon radiative transfer theory. Unlike steady state solutions obtained previously, time domain solutions will more closely correspond to experiments that use tone burst sources. In this paper, we discuss the time dependence of the backscattered longitudinal intensity from a polycrystalline medium excited by a normally incident longitudinal wave idealized as an impulsive deposition of energy. It is shown that multiple scattering effects become significant at times on the order of a mean free time or less. It is anticipated that this work may be applicable to microstructural characterization of polycrystalline, geophysical and other random media in which multiple scattering effects are important.

Submitted for publication to the *Journal of the Acoustical Society of America*

INTRODUCTION

Microstructural characterization of polycrystalline materials using diffuse or incoherent ultrasonic fields is becoming a powerful microstructural characterization tool.[1,2,3,4,5,6] Experiments involving diffuse fields, although requiring extensive spatial averaging, offer greater flexibility for in-situ measurements and require less stringent geometric conditions (e.g. parallel surfaces) than conventional coherent field measurements.[7,8,9,10,11] Researchers have thus far been successful in characterizing polycrystalline materials through measurements of the backscattered intensity. Some of the models developed to predict the backscattered intensity for polycrystalline materials have been based on single scattering assumptions which are valid for weakly scattering materials, early times, or instances when narrowly focussed beams are used.[4,5,6] Other models for the diffuse intensities are based on the diffusive limit in which the ultrasonic energy has scattered sufficiently many times that it can be modelled using a diffusion equation.[12,13] In many cases, however, the intermediate multiple scattering range is important. Unlike the singly scattered fields, the multiply scattered fields are sensitive to the angular dependence of the scattering amplitudes and to absorption as well as to scattering.

A method was recently presented to model the multiply scattered diffuse intensity of ultrasound in polycrystalline media.[13,14,15] This model includes all multiple scattering effects and thus covers the entire multiple scattering range from single scattering to the diffusive limit. It is based on radiative transfer theory[16,17,18,19] in which an ultrasonic radiative transfer equation (URTE) is derived. Thus far only steady state solutions of the URTE have been presented[14,15] which, ordinarily, do not reflect typical experiments that are currently performed with diffuse intensity. Such experiments are usually done in the time domain using short tone bursts. Time domain solutions to the URTE were briefly discussed by Turner and Weaver,[14] but none were presented. In this paper we discuss these temporal solutions due to a normally incident longitudinal wave idealized as an

impulsive deposition of longitudinal energy. It is shown that the full multiply scattered field exhibits behavior dramatically different than the singly scattered field, and that the effects of multiple scattering may be significant at times on the order of a mean free time or less.

The ultrasonic radiative transfer equation is presented and discussed in the next section. Section II contains the derivation of closed form solutions for the singly scattered intensities. In section III, we present numerical solutions for the complete backscattered longitudinal intensity as a function of time for the case of polycrystalline iron.

I. ULTRASONIC RADIATIVE TRANSFER THEORY

The ultrasonic radiative transfer equation (URTE) has been derived for a polycrystalline medium through an examination of ensemble averaged responses of the elastic wave equation by the use of the Bethe-Salpeter equation.[13,15] It is expected to be valid within the limit of its primary assumption that the material heterogeneity is weak. This criterion is satisfied by a large number of materials of common interest. The URTE governs the propagation of diffuse intensities and includes all multiple scattering effects.

The steady state solutions presented previously[14,15] exhibit many of the features expected for a multiple scattering model. In the limit of high absorption, the solution reduces to a single scattering solution. In the opposite limit, deep within the medium and after the intensities have scattered many times, the solution approaches a diffusive limit with the expected equipartitioning of energy.[13,20] Steady state solutions cannot, however, model the time domain behavior observed in current experimental work. This paper is concerned, therefore, with the extension of the previously developed theory to the case of time varying intensities. In this section the ultrasonic radiative transfer equation is presented with the time dependence retained.

It should be noted that this problem contains two distinct time scales which are Fourier transformed to two distinct frequencies. The *inner* frequency, ω, defines the excitation frequency which governs the elastic wave equation used for the derivation of the URTE. This frequency is typically of order several MHz. The *outer* frequency, Ω, typically of the order of several hundred kHz, defines the frequency which governs the much slower temporal evolution of the diffuse intensities governed by the URTE. In the assumed limit that the material heterogeneities are weak, these time scales are widely separated and the distinction between ω and Ω is legitimate.

The geometry of the problem to be discussed is shown in Fig. 1. The medium is invariant in the x and y directions and is semi-infinite in the z direction. A normally incident longitudinal wave with incident flux F_{L0} and delta function time dependence (as discerned on the outer scale) is used as the excitation input. On the inner time scale one may think of this input as a short tone burst with center frequency ω. With this axisymmetric incident field the intensity in the medium varies as a function of depth, time, and direction of propagation. This direction is given by μ, the cosine of the angle between the direction of the intensity of interest and the z axis. The intensity at $\mu < 0$ is in the upward direction out of the scattering medium and the intensity at $\mu > 0$ is in the downward direction, into the scattering medium.

As discussed previously,[14,15] the URTE for this problem may be written

$$\mu \frac{\partial \underline{I}(\tau,\xi,\mu)}{\partial \tau} + \underline{\underline{c}}^{-1} \frac{\partial \underline{I}(\tau,\xi,\mu)}{\partial \xi} + (\underline{\underline{\kappa}} + \underline{\underline{\upsilon}})\underline{I}(\tau,\xi,\mu) = \frac{1}{2\kappa_T}\int_{-1}^{+1} \underline{\underline{P}}(\mu;\mu')\underline{I}(\tau,\xi,\mu')d\mu' + \underline{S}_L(\mu,\mu_0)e^{-\tilde{\sigma}_L \tau/\mu_0}\delta(\xi - c_T\tau/c_L\mu_0), \tag{1}$$

where the Stokes vector, $\underline{I}$, contains the five elastic Stokes parameters, one longitudinal, I_L, and four shear, I_{SV}, I_{SH}, U, and V which completely characterize the diffuse intensity. The total intensity is obtained by including the incident wave also.

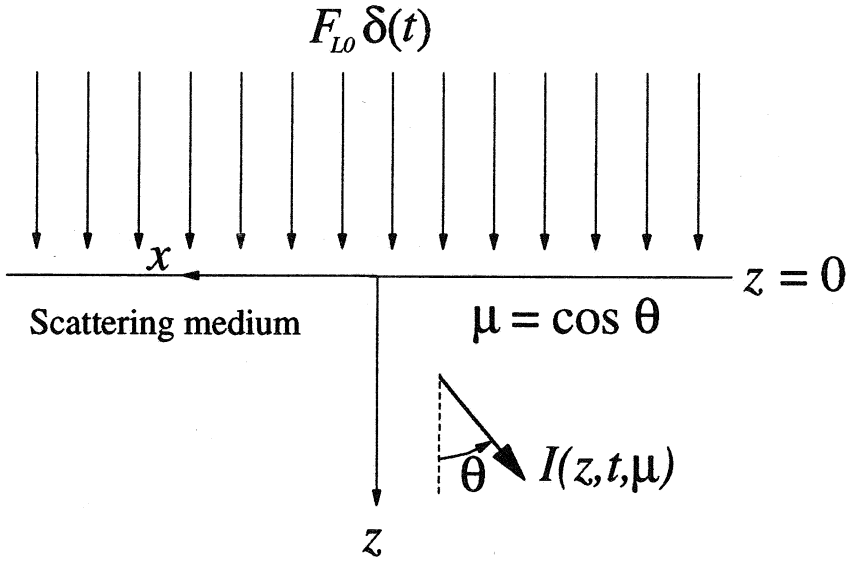

Figure 1. Geometry of the problem.

The incident direction μ_0 is +1.0. The matrices $\underline{\underline{\tilde{c}}}$, $\underline{\underline{\tilde{\kappa}}}$, and $\underline{\underline{\tilde{\upsilon}}}$ define the dimensionless wave speed, scattering, and absorption matrices which are given by

$$\underline{\underline{\tilde{c}}} = \begin{bmatrix} \frac{c_L}{c_T} & 0 & 0 & 0 & 0 \\ 0 & 1 & 0 & 0 & 0 \\ 0 & 0 & 1 & 0 & 0 \\ 0 & 0 & 0 & 1 & 0 \\ 0 & 0 & 0 & 0 & 1 \end{bmatrix}, \quad \underline{\underline{\tilde{\kappa}}} = \begin{bmatrix} \frac{\kappa_L}{\kappa_T} & 0 & 0 & 0 & 0 \\ 0 & 1 & 0 & 0 & 0 \\ 0 & 0 & 1 & 0 & 0 \\ 0 & 0 & 0 & 1 & 0 \\ 0 & 0 & 0 & 0 & 1 \end{bmatrix}, \quad \underline{\underline{\tilde{\upsilon}}} = \frac{1}{\kappa_T} \begin{bmatrix} \upsilon_L & 0 & 0 & 0 & 0 \\ 0 & \upsilon_T & 0 & 0 & 0 \\ 0 & 0 & \upsilon_T & 0 & 0 \\ 0 & 0 & 0 & \upsilon_T & 0 \\ 0 & 0 & 0 & 0 & \upsilon_T \end{bmatrix}, \quad (2)$$

where c_L and c_T, κ_L and κ_T, υ_L and υ_T are the wave speeds, intensity scattering attenuations, and intensity absorption attenuations for the longitudinal (L) and transverse (T) modes. The dimensionless total attenuations, $\tilde{\sigma}_L = (\kappa_L + \upsilon_L)/\kappa_T$ and $\tilde{\sigma}_T = 1 + \upsilon_T/\kappa_T$, include both scattering and absorption. The dimensionless depth, $\tau = \kappa_T z$, is measured in units of inverse shear intensity attenuation, while the dimensionless time, $\xi = c_T \kappa_T t$, is measured in units of shear intensity mean free time. The Mueller matrix, $\underline{\underline{P}}$, governs the scattering between each of the Stokes parameters. It contains combinations of inner products of the covariance of elastic moduli fluctuations and wave vectors. $\underline{\underline{P}}$ is also a

function of the spatial Fourier transform of the two-point correlation function of the material properties.[13,15] This matrix is parametrically dependent upon the inner frequency, ω, and is directly related to $\underline{\underline{\tilde{\kappa}}}$. It has been derived for polycrystalline aggregates with cubic[15] and hexagonal crystallites.[21]

The diffuse intensity has a source, $\underline{S}_L$, due to a normally incident ($\mu_0 = +1$) longitudinal wave. It is given by

$$\underline{S}_L(\mu, \mu_0 = +1) = \begin{Bmatrix} S_{LL} \\ \underline{S}_{LT} \end{Bmatrix} = \frac{F_{L0}}{2\kappa_T} \begin{Bmatrix} P_{11}(\mu;\mu_0 = +1) \\ P_{21}(\mu;\mu_0 = +1) \\ P_{31}(\mu;\mu_0 = +1) \\ P_{41}(\mu;\mu_0 = +1) \\ 0 \end{Bmatrix}, \tag{3}$$

and includes a contribution S_{LL} which is the singly scattered longitudinal to longitudinal part, and a contribution $\underline{S}_{LT}$ which is the remaining four-component vector containing the singly scattered longitudinal to shear parts. The delta function time dependence in the source term in Eq. (1) has a time shift to satisfy causality within the medium.

A Fourier transform pair may be defined which governs the transform between dimensionless outer time, ξ, and dimensionless outer frequency, Ω. This transform pair is

$$\underline{\tilde{I}}(\tau, \Omega, \mu) = \int_{-\infty}^{+\infty} \underline{I}(\tau, \xi, \mu) e^{-i\Omega\xi} d\xi, \qquad \underline{I}(\tau, \xi, \mu) = \frac{1}{2\pi} \int_{-\infty}^{+\infty} \underline{\tilde{I}}(\tau, \Omega, \mu) e^{i\Omega\xi} d\Omega. \tag{4}$$

With this transform definition, Eq. (1) becomes

$$\mu \frac{\partial \underline{\tilde{I}}(\tau, \Omega, \mu)}{\partial \tau} + \left(\underline{\underline{\tilde{\kappa}}} + \underline{\underline{\tilde{\upsilon}}} + i\Omega \underline{\underline{\tilde{c}}}^{-1} \right) \underline{\tilde{I}}(\tau, \Omega, \mu) = \frac{1}{2\kappa_T} \int_{-1}^{+1} \underline{\underline{P}}(\mu;\mu') \underline{\tilde{I}}(\tau, \Omega, \mu') d\mu' + \underline{S}_L(\mu, \mu_0 = +1) e^{-\tilde{\sigma}_L \tau/\mu_0 - i\Omega c_T \tau / c_L \mu_0}. \tag{5}$$

We discuss solutions of this equation in the next two sections. Solutions to other types of incident time histories may be found by convolution.

II. SINGLY SCATTERED SOLUTIONS

A single scattering assumption is often used with good success for materials with weak scattering, for early times, or for experiments involving focussed transducers.[4,5,6] The implication is that the intensity scatters only once before exiting the medium. The independent scatterer model[4] is one such model. The singly scattered intensity, using radiative transfer theory, is the solution to Eq. (5) with the integral term removed. This solution has been developed for the steady state case[14,18] in which $\Omega = 0$. Here we generalize that solution to the case $\Omega \neq 0$ and obtain the singly scattered solution as a function of the outer frequency due to an impulsive deposition of normally incident longitudinal energy. This solution is then analytically transformed back to the time domain and shown to be equivalent to the independent scatterer model.[4,5]

The singly scattered longitudinal intensity in the outer frequency domain in the upward ($\mu < 0$) and downward ($\mu > 0$) directions is the solution of Eq. (5) without the integral term[14,15]

$$\tilde{I}_L(\tau,\Omega,\mu<0) = \frac{S_{LL}e^{-\tilde{\sigma}_L\tau/\mu_0 - i\Omega c_T\tau/\mu_0 c_L}}{-\mu(1/\mu_0 - 1/\mu)(\tilde{\sigma}_L + i\Omega c_T/c_L)},$$
$$\tilde{I}_L(\tau,\Omega,\mu>0) = \frac{S_{LL}(e^{-\tilde{\sigma}_L\tau/\mu - i\Omega c_T\tau/c_L\mu} - e^{-\tilde{\sigma}_L\tau/\mu_0 - i\Omega c_T\tau/c_L\mu_0})}{\mu(1/\mu_0 - 1/\mu)(\tilde{\sigma}_L + i\Omega c_T/c_L)}. \quad (6)$$

The transverse intensities are given by

$$\underline{\tilde{I}}_T(\tau,\Omega,\mu<0) = \frac{\underline{S}_{LT}e^{-\tilde{\sigma}_L\tau/\mu_0 - i\Omega c_T\tau/c_L\mu_0}}{-\mu(\tilde{\sigma}_L/\mu_0 - \tilde{\sigma}_T/\mu + i\Omega(c_T/c_L\mu_0 - 1/\mu))},$$
$$\underline{\tilde{I}}_T(\tau,\Omega,\mu>0) = \frac{\underline{S}_{LT}(e^{-\tilde{\sigma}_T\tau/\mu - i\Omega\tau/\mu} - e^{-\tilde{\sigma}_L\tau/\mu_0 - i\Omega c_T\tau/c_L\mu_0})}{\mu(\tilde{\sigma}_L/\mu_0 - \tilde{\sigma}_T/\mu + i\Omega(c_T/c_L\mu_0 - 1/\mu))}. \quad (7)$$

The inverse transforms may be obtained by straightforward application of the Cauchy residue theorem. The resulting time dependent singly scattered intensities are

$$I_L(\tau,\xi,\mu<0)=\frac{S_{LL}c_L e^{-\tilde{\sigma}_L c_L \xi/c_T}}{-\mu c_T(1/\mu_0-1/\mu)}H(\xi-c_T\tau/c_L\mu_0),$$

$$I_L(\tau,\xi,\mu>0)=\frac{S_{LL}c_L e^{-\tilde{\sigma}_L c_L \xi/c_T}}{\mu c_T(1/\mu_0-1/\mu)}[H(\xi-c_T\tau/c_L\mu)-H(\xi-c_T\tau/c_L\mu_0)], \tag{8}$$

and

$$\underline{I}_T(\tau,\xi,\mu<0)=\frac{\underline{S}_{LT}e^{-\tau\tilde{\sigma}_L/\mu_0}e^{-\zeta_{LT}(\xi-c_T\tau/c_L\mu_0)}}{-\mu(c_T/c_L\mu_0-1/\mu)}H(\xi-c_T\tau/c_L\mu_0),$$

$$\underline{I}_T(\tau,\xi,\mu>0)=\frac{\underline{S}_{LT}e^{-\tau\tilde{\sigma}_L/\mu_0}e^{-\zeta_{LT}(\xi-c_T\tau/c_L\mu_0)}}{\mu(c_T/c_L\mu_0-1/\mu)}[H(\xi-\tau/\mu_0)-H(\xi-c_T\tau/c_L\mu_0)], \tag{9}$$

where we have defined

$$\zeta_{LT}=\frac{(\tilde{\sigma}_L/\mu_0-\tilde{\sigma}_T/\mu)}{(c_T/c_L\mu_0-1/\mu)} \tag{10}$$

for convenience. This quantity, ζ_{LT}, is the pole of Eqs. (7) divided by $i=\sqrt{-1}$. It governs the temporal decay of the mode converted ray and is equal to the total travel path attenuation divided by the inverse of the total wave speed along the travel path. Thus, ζ_{LT} is related to the inverse amount of time a mode converted ray takes to scatter. *H(x)* is the Heaviside Step Function which is equal to unity for *x>0*.

Using Eq. (8) we can write the solution to the singly scattered longitudinal intensity in the backscatter ($\mu=-1$) direction at the surface of the material ($\tau=0$) as,

$$I_L(\tau=0,\xi,\mu=-1)=\frac{c_L}{4c_T\kappa_T}P_{11}(\mu=-1;\mu_0=+1)e^{-\tilde{\sigma}_L c_L\xi/c_T}H(\xi), \tag{11}$$

where the definition of S_{LL} given in Eq. (3) has been used. If the definition of P_{11} for cubic crystallites is used,[15] evaluated at $\mu_0=+1$ and $\mu=-1$ we find that

$$I_L(\tau=0,\xi,\mu=-1)=\frac{c_L}{4c_T\kappa_T}\frac{32\beta\nu^2}{525\rho^2c_L^4}\frac{x_L^4}{[1+(2x_L)^2]^2}e^{-\tilde{\sigma}_L c_L\xi/c_T}H(\xi), \tag{12}$$

where $\nu = C_{11} - C_{12} - 2C_{44}$ is the crystallite anisotropy and $x_L = \omega/c_L\beta$ is a dimensionless measure of inner frequency. An exponential two-point correlation function of the form $e^{-\beta r}$ has also been assumed where β is a measure of the length scale. The amplitude of the backscattered longitudinal intensity has the same frequency, time, and material dependence as the backscattered power given by Rose[5] using independent scatterer theory. Thus, the independent scatterer model may be considered to be a limiting case of the URTE.

III. MULTIPLY SCATTERED SOLUTIONS

Solutions to the entire URTE given in Eq. (5) must be obtained numerically for a given excitation frequency, ω.[14] The discrete ordinates method[14,16,18] was used to solve the URTE in outer frequency space. The resulting intensities were then numerically transformed back to the outer time domain.

The Mueller matrix, $\underline{\underline{P}}$, was obtained by assuming an exponential two-point correlation function as discussed above and elsewhere.[13,15] Using parameters corresponding to polycrystalline iron, the dimensionless crystallite anisotropy, $\nu/\rho c_T = -1.66$ and $c_L/c_T = 1.827$. Results for the multiply scattered longitudinal intensity in the backscatter direction ($\mu = -1$) are shown in Fig. 2 as a function of dimensionless time, $\xi = c_T\kappa_T t$ at a dimensionless inner frequency of $x_T = \omega/c_T\beta = 0.5$. Each curve was calculated at a different absorption rate using the dimensionless absorption defined as the ratio of the absorption attenuation to the scattering attenuation, $\tilde{\upsilon}_T = \upsilon_T/\kappa_T$. The absorption per wavelength for the different modes was assumed equal which implies that $c_L\upsilon_L = c_T\upsilon_T$. The absorption would normally be frequency dependent, but for simplicity, it is given here as a fraction of the scattering attenuation.

The results show that the multiply scattered intensity is equal to the singly scattered intensity at early times as expected. After only a few mean free times, however, the multiply scattered solution has deviated sharply from the singly scattered solution. The

multiply backscattered intensity quickly rises to a peak and then begins an asymptotic decay. As the absorption is increased, the multiply scattered solution approaches the absorptive singly scattered solution as expected. In this case, multiple scattering effects are quickly dampened out.

The peak in these solutions was rather unexpected. The energy that arrives before this peak has a large single scattering component. After the peak, however, the signal contains almost no singly scattered energy. The arrival time of the peak is also a function of the wave speed ratio, listening direction, and inner frequency. In fact, as the wave speeds become less disparate this peak arrives earlier in time and can become nonexistent. In this case, the intensity begins at its peak value and then decays. Thus, this peak may be due to the attenuation ratio which allows the incident longitudinal energy to penetrate deeper than the shear energy which delays the return of that energy to the surface. The unexpected peak and additional structure of the multiply scattered solution underscore the added microstructural information available in multiply scattered fields compared with the singly scattered fields.

Figure 3 shows the backscattered intensity for iron at a higher dimensionless excitation frequency, $x_T = 3.0$. The results are similar, except for the location of the peak in the multiply scattered solution. The peak now occurs at about 21 shear mean free times for zero absorption after almost all of the singly scattered energy has decayed. The shift of this peak is due to the directional dependence of the scattering. The greater amount of forward scattering that occurs at the higher frequency,[15] delays the time for much of the energy to be multiply scattered into the backward direction. This directionality of the scattering also amplifies the effects of absorption. The high frequency results with absorption deviate more quickly from the zero absorption solution than the low frequency results of Fig. 2.

The results shown in Figs. 2 and 3 have similar trends. They begin at the single scattering solution, rise to some maximum, and then reach an asymptotically decaying limit. This late time behavior is expected to correspond to the diffusion limit where the energy is nearly isotropic and equipartitioned.[13,20] The approach to the diffusive limit and the validity of the diffusion approximation are topics for a future communication.

The angular dependence of the backscatter peak is shown in Figs. 4 and 5 for x_T = 0.5 and x_T = 3.0, respectively. The results are the upward longitudinal intensity in three directions: 0°, 48.5°, and 76.2° from vertical. The low frequency results display the general isotropic scattering nature expected. The energy peaks do not arrive at precisely identical times, but the peaks are fairly closely spaced in time. At the higher frequency, shown in Fig. 5, these peaks are distinctly separated. The separation between the peaks alludes to the time for the forward scattered energy to return to the backscatter direction. The arrival time of these peaks as a function of direction provides insight into the directional tendency of the scattering functions which govern the multiple scattering process.

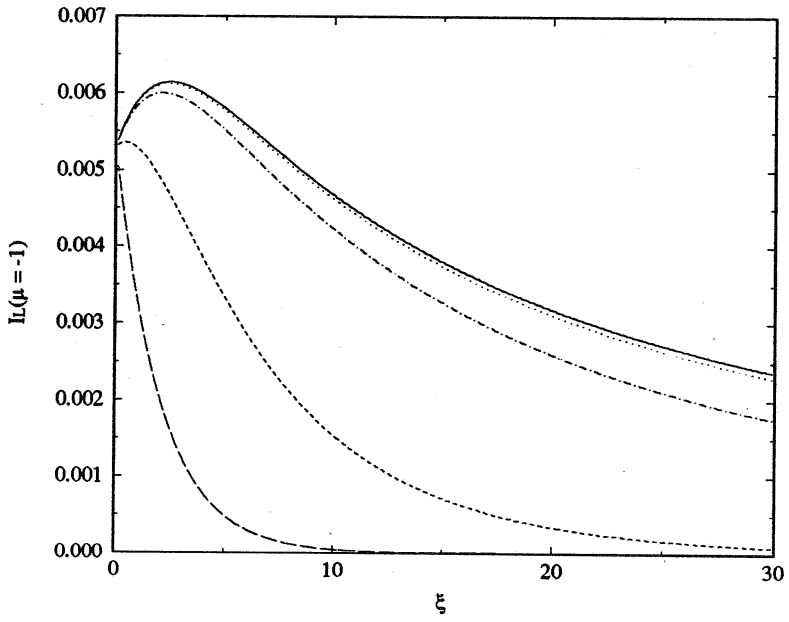

Figure 2. Backscattered ($\mu = -1$) longitudinal intensity vs. dimensionless time at dimensionless inner frequency $x_T = 0.5$ for different absorption rates: no absorption (solid line), $\tilde{\upsilon}_T$ = .001 (dotted), $\tilde{\upsilon}_T$ = .01 (dot dash), $\tilde{\upsilon}_T$ = .111 (small dash). The singly scattered solution without absorption (Eq. (8)) is shown by the large dashes.

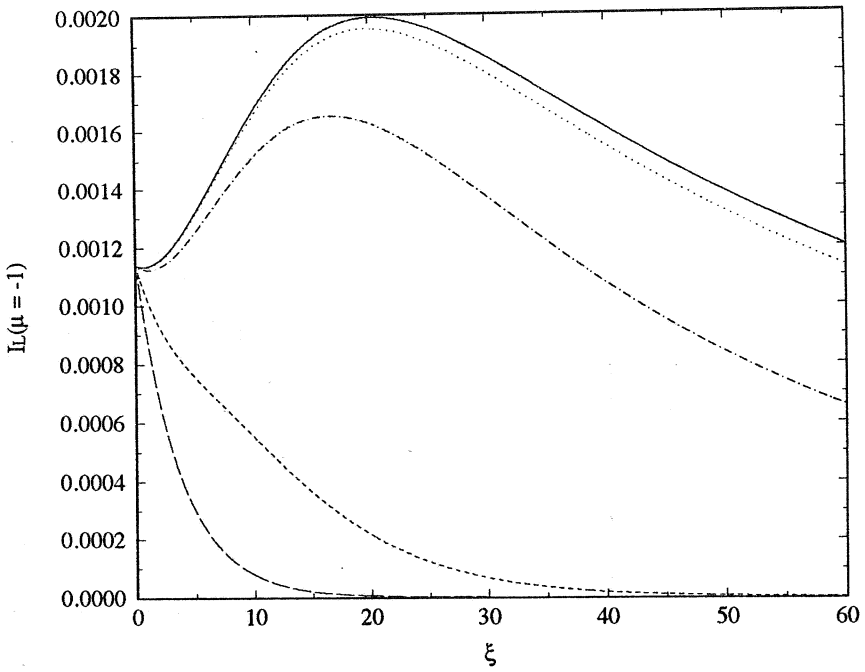

Figure 3. Backscattered ($\mu = -1$) longitudinal intensity vs. dimensionless time at dimensionless inner frequency $x_T = 3.0$ for different absorption rates: no absorption (solid line), $\tilde{\upsilon}_T$ = .001 (dotted), $\tilde{\upsilon}_T$ = .01 (dot dash), $\tilde{\upsilon}_T$ = .111 (small dash). The singly scattered solution without absorption (Eq. (8)) is shown by the large dashes.

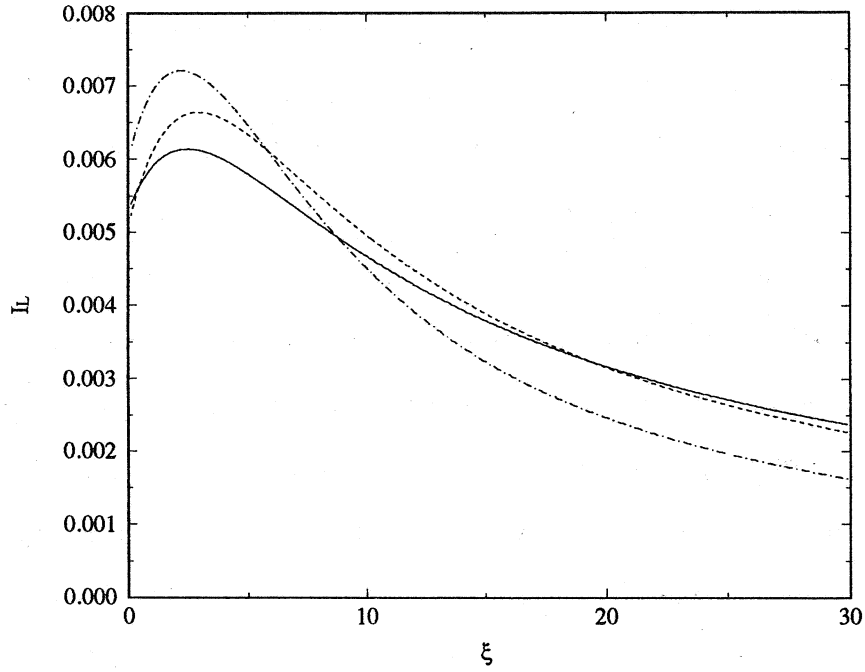

Figure 4. Upward longitudinal intensity vs. dimensionless time at dimensionless inner frequency $x_T = 0.5$ in three different directions: 0° (solid line), 48.5° (dashed), and 76.2° (dot-dash) from vertical.

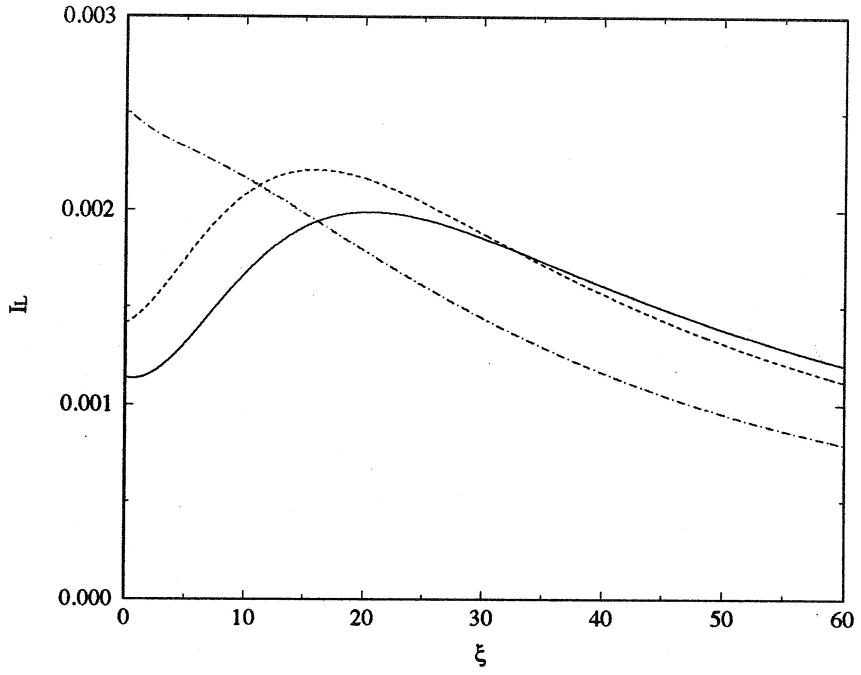

Figure 5. Upward longitudinal intensity vs. dimensionless time at dimensionless inner frequency $x_T = 3.0$ in three different directions: 0° (solid line), 48.5° (dashed), and 76.2° (dot-dash) from vertical.

The time for the multiply scattered intensity to be significant in comparison with the singly scattered intensity can also be examined. After a certain amount of time, the multiple scattering effects will be of primary importance. These results can be put into dimensional units for greater clarity. Table I contains the time for the multiply scattered intensity to be twice that of the singly scattered. Two materials are considered: iron which scatters strongly and aluminum which is a much weaker scattering medium ($\nu/\rho c_T^2 = -0.412$). The respective mean free times for each material defined as $1/c\kappa$ are shown in Table II. The results from the solution of the URTE agree with intuition. The time for multiple scattering to dominate occurs between the longitudinal and shear mean free times. For lower frequencies this multiple scattering critical time is closer to the longitudinal mean free time. At higher frequencies this critical time shifts towards the shear mean free time. This result highlights the complications that arise as a result of the presence of two propagation modes with different wave speeds. It is also unclear which mean free time is the more important of the two. One should keep in mind, though, that

at times earlier than either mean free time, the multiple scattering effects can be significantly greater than the singly scattered energy as Figs. 2 and 3 reveal. Thus, examinations of mean free times may not be enough for determining applicability of the single scattering approximation.

Table I. Time for the multiply scattered longitudinal intensity to be twice the singly scattered intensity for iron and aluminum at two frequencies with $\beta = 10/\text{mm}$.

f (MHz)	Fe	Al
2.5	8.65 μs	155 μs
15	0.241	5.58

Table II. Mean free times ($1/c\kappa$) for iron and aluminum for both propagation modes.

Mean Free Times ($1/c\kappa$)			
f (MHz)		Fe	Al
2.5	L	15.1 μs	309 μs
	T	7.18	122
15	L	0.363	8.43
	T	0.0977	1.65

IV. DISCUSSION

Results have been presented for the multiply scattered solution in the time domain for ultrasonic scattering in a polycrystalline medium using ultrasonic radiative transfer theory. The multiply scattered solutions have very different behavior than the singly scattered solutions and contain additional microstructural information. It was also shown that multiple scattering effects may be significant at times on the order of a mean free

time or less.

One should keep in mind that the results presented here are for a plane wave at normal incidence. Experiments involving focussed transducers have been modeled well using single scattering models for materials that scatterer strongly. In these cases, multiple scattering effects are minimized by the finite beam width which allows very little of the multiply scattered energy to reenter the beam. However, as the beam focus is placed farther into the medium or as one examines later times, one would expect the multiple scattering effects to become more pronounced.

Boundary reflection effects, which are important in typical experiments performed in a water bath, have not been included thus far in this work. Inclusion of these effects into the URTE will be the subject of a later communication.

ACKNOWLEDGMENT

This work was sponsored by the National Science Foundation, Grant No. MSS-91-14360.

REFERENCES

1. J. Saniie and N. M. Bilgutay, "Quantitative grain size evaluation using ultrasonic backscattered echoes," *J. Acoust. Soc. Am.* **80**, 1816-1824 (1986).

2. B. Fay, "Theoretical considerations of ultrasound backscatter," (in German) *Acustica* **28**, 354-357 (1973).

3. K. Goebbels, "Ultrasonics for microcrystalline structure examination," *Phil. Trans. R. Soc. Lond. A* **320**, 161-169 (1986).

4. F. J. Margetan, T. A. Gray, and R. B. Thompson, "A technique for quantitatively measuring microstructurally induced ultrasonic noise," *Review of Progress in Quantitative NDE, 10,* edited by D. O. Thompson and D. E. Chimenti (Plenum Press, New York, 1991) pp. 1721-1728.

5. J. H. Rose, "Ultrasonic backscatter from microstructure," *Review of Progress in Quantitative NDE, 11,* edited by D. O. Thompson and D. E. Chimenti (Plenum Press, New York, 1992) pp. 1677-1684.

6. M. D. Russell and S. P. Neal, "Grain noise power spectrum estimation for normal incidence ultrasonic interrogation of weak scattering polycrystalline materials using experimentally estimated longitudinal-wave backscatter coefficients," to be published in *Ultrasonics*.

7. W. P. Mason and H. J. McSkimm, "Attenuation and scattering of high frequency sound waves in metals and glasses," *J. Acoust. Soc. Am.* **19**, 464-473 (1947).

8. A. B. Bhatia, "Scattering of high-frequency sound waves in polycrystalline materials," *J. Acoust. Soc. Am.* **19**, 16-23 (1959).

9. E. P. Papadakis, "Scattering in polycrystalline media," *Meth. Exp. Phys.* **19**, 237-298 (1981).

10. D. W. Fitting and L. Adler, *Ultrasonic Spectral Analysis for Nondestructive Evaluation* (Plenum Press, New York, 1981).

11. A. Vary, "Ultrasonic measurement of material properties," *Research Techniques in Nondestructive Testing V. IV,* edited by R. S. Sharpe (Academic Press, New York, 1980) pp. 159-204.

12. C. B. Guo, P. Holler, and K. Goebbels, "Scattering of ultrasonic waves in anisotropic polycrystalline metals," *Acustica* **59**, 112-120 (1985).

13. R. L. Weaver, ''Diffusivity of ultrasound in polycrystals,'' *J. Mech. Phys. Solids* **38**, 55-86 (1990).

14. J. A. Turner and R. L. Weaver, ''Radiative transfer of ultrasound,'' TAM Report No. 725, University of Illinois, September, 1993; J. A. Turner and R. L. Weaver, ''Radiative transfer of ultrasound,'' submitted to *J. Acoust. Soc. Am.*

15. J. A. Turner and R. L. Weaver, ''Radiative transfer and multiple scattering of diffuse ultrasound in polycrystalline media,'' TAM Report No. 738, University of Illinois, November, 1993; J. A. Turner and R. L. Weaver, ''Radiative transfer and multiple scattering of diffuse ultrasound in polycrystalline media,'' submitted to *J. Acoust. Soc. Am.*

16. S. Chandrasekhar, *Radiative Transfer* (Dover, New York, 1960).

17. V. V. Sobolev, *A Treatise on Radiative Transfer* (D. Van Nostrand, New Jersey, 1963).

18. A. Ishimaru, *Wave Propagation and Scattering in Random Media* (Academic Press, New York, 1978), Vol. 1.

19. Tsang, L., J. A. Kong, and R. T. Shin, *Theory of Microwave Remote Sensing* (John Wiley and Sons, New York, 1985).

20. Weaver, R. L., ''On diffuse waves in solid media,'' *J. Acoust. Soc. Am.* **71**, 1608-1609 (1982).

21. Turner, J. A., ''Radiative transfer of ultrasound,'' Ph.D. Thesis, Department of Theoretical and Applied Mechanics, University of Illinois, (1994).

List of Recent TAM Reports

No.	Authors	Title	Date
705	Stewart, D. S., and J. B. Bdzil	Asymptotics and multi-scale simulation in a numerical combustion laboratory	Jan. 1993
706	Hsia, K. J., Y.-B. Xin, and L. Lin	Numerical simulation of semi-crystalline nylon 6: Elastic constants of crystalline and amorphous parts	Jan. 1993
707	Hsia, K. J., and J. Q. Huang	Curvature effects on compressive failure strength of long fiber composite laminates	Jan. 1993
708	Jog, C. S., R. B. Haber, and M. P. Bendsøe	Topology design with optimized, self-adaptive materials	Mar. 1993
709	Barkey, M. E., D. F. Socie, and K. J. Hsia	A yield surface approach to the estimation of notch strains for proportional and nonproportional cyclic loading	Apr. 1993
710	Feldsien, T. M., A. D. Friend, G. S. Gehner, T. D. McCoy, K. V. Remmert, D. L. Riedl, P. L. Scheiberle, and J. W. Wu	Thirtieth student symposium on engineering mechanics, J. W. Phillips, coord.	Apr. 1993
711	Weaver, R. L.	Anderson localization in the time domain: Numerical studies of waves in two-dimensional disordered media	Apr. 1993
712	Cherukuri, H. P., and T. G. Shawki	An energy-based localization theory: Part I—Basic framework	Apr. 1993
713	Manring, N. D., and R. E. Johnson	Modeling a variable-displacement pump	June 1993
714	Birnbaum, H. K., and P. Sofronis	Hydrogen-enhanced localized plasticity—A mechanism for hydrogen-related fracture	July 1993
715	Balachandar, S., and M. R. Malik	Inviscid instability of streamwise corner flow	July 1993
716	Sofronis, P.	Linearized hydrogen elasticity	July 1993
717	Nitzsche, V. R., and K. J. Hsia	Modelling of dislocation mobility controlled brittle-to-ductile transition	July 1993
718	Hsia, K. J., and A. S. Argon	Experimental study of the mechanisms of brittle-to-ductile transition of cleavage fracture in silicon single crystals	July 1993
719	Cherukuri, H. P., and T. G. Shawki	An energy-based localization theory: Part II—Effects of the diffusion, inertia and dissipation numbers	Aug. 1993
720	Aref, H., and S. W. Jones	Chaotic motion of a solid through ideal fluid	Aug. 1993
721	Stewart, D. S.	Lectures on detonation physics: Introduction to the theory of detonation shock dynamics	Aug. 1993
722	Lawrence, C. J., and R. Mei	Long-time behavior of the drag on a body in impulsive motion	Sept. 1993
723	Mei, R., J. F. Klausner, and C. J. Lawrence	A note on the history force on a spherical bubble at finite Reynolds number	Sept. 1993
724	Qi, Q., R. E. Johnson, and J. G. Harris	A re-examination of the boundary layer attenuation and acoustic streaming accompanying plane wave propagation in a circular tube	Sept. 1993
725	Turner, J. A., and R. L. Weaver	Radiative transfer of ultrasound	Sept. 1993
726	Yogeswaren, E. K., and J. G. Harris	A model of a confocal ultrasonic inspection system for interfaces	Sept. 1993
727	Yao, J., and D. S. Stewart	On the normal detonation shock velocity–curvature relationship for materials with large activation energy	Sept. 1993
728	Qi, Q.	Attenuated leaky Rayleigh waves	Oct. 1993
729	Sofronis, P., and H. K. Birnbaum	Mechanics of hydrogen–dislocation–impurity interactions: Part I—Increasing shear modulus	Oct. 1993
730	Hsia, K. J., Z. Suo, and W. Yang	Cleavage due to dislocation confinement in layered materials	Oct. 1993
731	Acharya, A., and T. G. Shawki	A second-deformation-gradient theory of plasticity	Oct. 1993

(continued on next page)

List of Recent TAM Reports (cont'd)

No.	*Authors*	*Title*	*Date*
732	Michaleris, P., D. A. Tortorelli, and C. A. Vidal	Tangent operators and design sensitivity formulations for transient nonlinear coupled problems with applications to elasto-plasticity	Nov. 1993
733	Michaleris, P., D. A. Tortorelli, and C. A. Vidal	Analysis and optimization of weakly coupled thermo-elasto-plastic systems with applications to weldment design	Nov. 1993
734	Ford, D. K., and D. S. Stewart	Probabilistic modeling of propellant beds exposed to strong stimulus	Nov. 1993
735	Mei, R., R. J. Adrian, and T. J. Hanratty	Particle dispersion in isotropic turbulence under the influence of non-Stokesian drag and gravitational settling	Nov. 1993
736	Dey, N., D. F. Socie, and K. J. Hsia	Static and cyclic fatigue failure at high temperature in ceramics containing grain boundary viscous phase: Part I—Experiments	Nov. 1993
737	Dey, N., D. F. Socie, and K. J. Hsia	Static and cyclic fatigue failure at high temperature in ceramics containing grain boundary viscous phase: Part II—Modelling	Nov. 1993
738	Turner, J. A., and R. L. Weaver	Radiative transfer and multiple scattering of diffuse ultrasound in polycrystalline media	Nov. 1993
739	Qi, Q., and R. E. Johnson	Resin flows through a porous fiber collection in pultrusion processing	Dec. 1993
740	Weaver, R. L., W. Sachse, and K. Y. Kim	Transient elastic waves in a transversely isotropic plate	Dec. 1993
741	Zhang, Y., and R. L. Weaver	Scattering from a thin random fluid layer	Dec. 1993
742	Weaver, R. L., and W. Sachse	Diffusion of ultrasound in a glass bead slurry	Dec. 1993
743	Sundermeyer, J. N., and R. L. Weaver	On crack identification and characterization in a beam by nonlinear vibration analysis	Dec. 1993
744	Li, L., and N. R. Sottos	Predictions of static displacements in 1–3 piezocomposites	Dec. 1993
745	Jones, S. W.	Chaotic advection and dispersion	Jan. 1994
746	Stewart, D. S., and J. Yao	Critical detonation shock curvature and failure dynamics: Developments in the theory of detonation shock dynamics	Feb. 1994
747	Mei, R., and R. J. Adrian	Effect of Reynolds-number-dependent turbulence structure on the dispersion of fluid and particles	Feb. 1994
748	Liu, Z.-C., R. J. Adrian, and T. J. Hanratty	Reynolds-number similarity of orthogonal decomposition of the outer layer of turbulent wall flow	Feb. 1994
749	Barnhart, D. H., R. J. Adrian, and G. C. Papen	Phase-conjugate holographic system for high-resolution particle image velocimetry	Feb. 1994
750	Qi, Q., W. D. O'Brien Jr., and J. G. Harris	The propagation of ultrasonic waves through a bubbly liquid into tissue: A linear analysis	Mar. 1994
751	Mittal, R., and S. Balachandar	Direct numerical simulation of flow past elliptic cylinders	May 1994
752	Anderson, D. N., J. R. Dahlen, M. J. Danyluk, A. M. Dreyer, K. M. Durkin, J. J. Kriegsmann, J. T. McGonigle, and V. Tyagi	Thirty-first student symposium on engineering mechanics, J. W. Phillips, coord.	May 1994
753	Thoroddsen, S. T.	The failure of the Kolmogorov refined similarity hypothesis in fluid turbulence	May 1994
754	Turner, J. A., and R. L. Weaver	Time dependence of multiply scattered diffuse ultrasound in polycrystalline media	June 1994